

Nonlinear Dynamics of Confined Polymer Melts with Attractive Walls

Yogesh M. Joshi*

Department of Chemical Engineering, Indian Institute of Technology–Kanpur,
Kanpur 208016, India

Received June 13, 2005. In Final Form: August 13, 2005

A scaling model is presented to analyze the reversible strain-hardening phenomenon in end-tethered polymer clay nanocomposites (Krishnamoorti, R.; Giannelis, E. P. *Langmuir* **2001**, *17*, 1448). It is assumed that for attractive clay–polymer interactions a fraction of the polymer chains that span the space between opposite clay plates get adsorbed on them, thereby bridging the plates. Under large amplitude oscillatory shear, such bridges are stretched, and this results in the strain-hardening behavior. The onset of strain hardening is predicted to be dependent only on the average distance separating the two plates and is independent of the frequency of the oscillations and the polymer molecular weight.

1. Introduction

In the past decade, polymer–clay nanocomposites have received significant attention because of their improved mechanical, thermal, and barrier properties.¹ Recently, there has been a lot of interest in synthesizing polymer-grafted clay nanocomposites by in situ polymerization because this technique results in better compatibility between the clay and the polymer and improved dispersion of the clay platelets.² The dynamics of layered silicate nanocomposites is dictated by the degree of dispersion of clay plates in the polymer matrix. Even for moderate concentrations of the clay, the space between the clay plates achieves macromolecular dimensions, and that makes it a model system to study the dynamics of polymer melts in confined geometries. In this letter, we analyze various rheological experiments performed by Krishnamoorti and Giannelis³ on an end-tethered polymer–clay nanocomposite⁴ that shows reversible strain hardening under large amplitude oscillatory shear (LAOS) flow. This behavior is particularly interesting because not many uncrosslinked systems show reversible strain hardening in shear flow.

Confined polymeric liquids are known to show qualitatively different flow behaviors compared to the bulk. Pioneering theoretical work on the nonlinear rheology of confined polymer molecules has been carried out by Subbotin and co-workers.^{5,6} In a series of papers, they presented scaling theories for polymer melts confined between walls that were molecular distances apart where the polymer chain bridges two opposite walls and also forms loops. They analyzed steady⁵ as well as nonlinear oscillatory⁶ shear flow with strong and weak adsorption

of the polymer chains having a coil size greater than the confinement distance. Furthermore, the surface coverage was considered to be small enough that the chains obey the Gaussian configuration. Under shear deformation, depending on the strength of the polymer–surface interactions, the bridge gets stretched or detached. Although their analysis does not show the strain hardening explicitly, it predicts rheological scaling relations for various regimes of steady and oscillatory shear flow fields.

Krishnamoorti and Giannelis³ studied the melt rheology of poly(ϵ -caprolactone)–montmorillonite clay nanocomposites of various clay concentrations. Under LAOS, the nanocomposite showed an unusual strain-hardening behavior in which the strain at the onset of strain hardening was independent of the polymer molecular weight and the frequency of oscillations but decreased with increasing clay concentration. The observed increase in complex viscosity was accompanied by a decrease in $\tan \delta$, suggesting a corresponding increase in the storage modulus. The phenomenon was reversible and showed slight hysteresis. Interestingly, when the nanocomposite was diluted with an equal amount of toluene, strain softening was observed with its onset decreasing with increasing frequency.³

We present a simple scaling model to analyze the observed phenomenon. We argue that a fraction of chains present in the clay galleries (space between the clay plates) get adsorbed on the surfaces of opposite clay plates and bridge them. Under LAOS, these bridges stretch to show strain hardening.

2. Analysis

Let us consider a polymer–clay nanocomposite system in which the clay plates are well dispersed (exfoliated) in the polymer matrix. The thickness of an individual clay plate is $t \approx 1$ nm with an aspect ratio of 100–1000. Sufficient preshearing of the system orients the surface normal of the clay plates in the direction of the velocity gradient.³ Let the average distance separating two neighboring clay plates be h . Figure 1 shows a slice of a system in a plane normal to the plane of the clay plates. In this Figure, we have shown an idealized scenario where all of the plates are equidistant. Because the clay plates have a finite aspect ratio, in one layer of thickness t , only a fraction of the area will be covered by the clay plates. If the volume fraction of clay is Φ and a fraction of area

* E-mail: joshi@iitk.ac.in. Tel: +91 512 259 7993. Fax: +91 512 259 0104.

(1) Giannelis, E. P.; Krishnamoorti, R.; Manias, E. D. *Adv. Polym. Sci.* **1998**, *138*, 107. Alexandre, M.; Dubois, P. *Mater. Sci. Eng.* **2000**, *R28*, 1.

(2) Lepoittevin, B.; Pantoustier, N.; Alexandre, M.; Calberg, C.; Jerome, R.; Dubois, P. *J. Mater. Chem.* **2002**, *12*, 3528. Shah, D.; Fytas, D.; Vlassopoulos, D.; Di, J.; Sogah, D.; Giannelis, E. P. *Langmuir* **2005**, *21*, 19.

(3) Krishnamoorti, R.; Giannelis, E. P. *Langmuir* **2001**, *17*, 1448.

(4) Messersmith, P. B.; Giannelis, E. P. *J. Polym. Sci., Part A: Polym. Chem.* **1995**, *33*, 1047.

(5) Subbotin, A.; Semenov, A.; Manias, G.; Hadziioannou, G.; ten Brinke, G. *Macromolecules* **1995**, *28*, 1511. Subbotin, A.; Semenov, A.; Hadziioannou, G.; ten Brinke, G. *Macromolecules* **1995**, *28*, 3901.

(6) Subbotin, A.; Semenov, A.; Hadziioannou, G.; ten Brinke, G. *Macromolecules* **1996**, *29*, 1296.

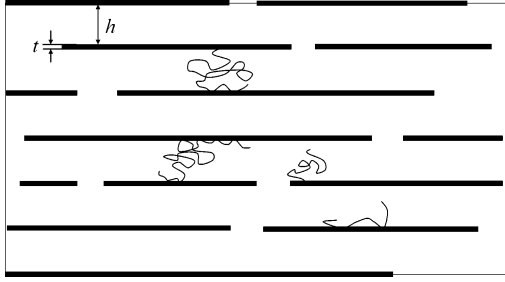


Figure 1. Slice of a system in a plane normal to the plane of clay plates. We have assumed that in one layer of thickness of t the fraction of area occupied by clay plates is given by ζ .

occupied by the clay plates is ζ , then h is given by

$$h = \frac{\zeta - \Phi}{\Phi} t \quad (1)$$

Although the explicit dependence of ζ on Φ is not known, it is expected to be monotonic. Furthermore, we anticipate that as $\Phi \rightarrow 0$, $\zeta \rightarrow 0$ and as $\Phi \rightarrow 1$, $\zeta \rightarrow 1$. We assume that their dependence has the following form:

$$\zeta = \Phi^\beta \quad (2)$$

Because clay layers are aligned, in the limit of $\Phi \rightarrow 0$, the introduction of additional clay plates in the system increases ζ more rapidly than Φ . Thus in the limit of $\Phi \rightarrow 0$, it is expected that $d\zeta/d\Phi > 1$. Furthermore, as $\Phi \rightarrow 1$, ζ linearly increases with increasing Φ . This makes β dependent on Φ ; that is, as $\Phi \rightarrow 0$, $\beta < 1$ and as $\Phi \rightarrow 1$, $\beta \rightarrow 1$. However, in this letter, because we are dealing with very small values of Φ (up to only 0.05), we assume β to be a constant with its value smaller than 1.

By combining eqs 1 and 2 we get

$$h = (\Phi^\beta - 1)t = [(1 + \xi)^{1-\beta} - 1]t \quad (3)$$

where ξ is the ratio of the volume of polymer to that of clay and is given by

$$\xi = \frac{1 - \Phi}{\Phi} = \frac{(1 - \phi)\rho_c}{\phi\rho_p} \quad (4)$$

Here, ϕ is the weight fraction of clay and is given by

$$\phi = \frac{\Phi\rho_c}{(1 - \Phi)\rho_p + \Phi\rho_c} \quad (5)$$

where ρ_c is the density of the clay plate and ρ_p is the density of the polymer melt. The overall picture of the system is shown in Figure 1. Because the space between the two clay plates is filled with polymer chains, the fraction of chains having a coil size greater than h can bridge the clay plates by getting adsorbed on them provided that the polymer–clay interactions are sufficiently attractive.

We now develop a model that resembles the experimental system. Figure 2 shows a schematic of a polymer chain undergoing deformation in an LAOS experiment. We consider two clay surfaces separated by a distance h . A gallery is assumed to contain unentangled monodispersed chains having a Gaussian configuration with a coil size greater than h . The polymer chains are assumed to bridge the two opposite clay surfaces and also form loops on both of the surfaces. Let the part of the polymer chain that forms the bridge have N_b segments of length a_s such that at equilibrium $h = a_s N_b^{0.5}$. Now let the system be subjected to a large amplitude oscillatory shear de-

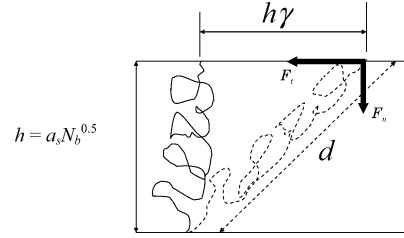


Figure 2. Schematic of the polymer chain bridging two opposite layers. The stretching of the same under LAOS can also be seen.

formation with angular frequency ω and a time-dependent strain $\gamma = \gamma_0 \sin \omega\tau$, where τ is time. If d is the average end-to-end distance of the bridge, then from Figure 2 we get $d^2 = h^2(\gamma^2 + 1)$. Assuming the polymer bridge to be a nonlinear spring, the tension in the spring is given by⁵

$$f = \frac{3kTd}{h^2} \varphi\left(\frac{d}{a_s N_b}\right) = \frac{3kTd}{h^2} \left(1 + c_1 \frac{d^2}{a_s^2 N_b^2} + \dots\right) \dots \quad d < a_s N_b \quad (6)$$

where $c_i > 0$ ($i = 1, 2, 3, \dots$) are numerical coefficients, k is the Boltzmann constant, and T is the temperature. Resolving the force into normal and tangential directions, we get

$$f_n(\gamma) = \frac{3kT}{h} \left(1 + c_1 \frac{d^2}{a_s^2 N_b^2} + \dots\right), \quad f_t(\gamma) = \frac{3kT}{h} \gamma \left(1 + c_1 \frac{d^2}{a_s^2 N_b^2} + \dots\right) \quad (7)$$

If τ_0 is a characteristic relaxation time (lifetime) of a bridge, then for frequencies $\omega > 1/\tau_0$ the bridge does not detach in the imposed time scale.⁶ As the strain increases, the bridge gets elongated and contributes to the storage modulus (G') and loss modulus (G''). Neglecting the higher-order harmonics,^{3,6} G' and G'' can be written as

$$G' = \frac{\bar{\sigma} f_t(\gamma_0)}{\gamma_0} = \frac{3kT}{h} \bar{\sigma} \left(1 + c_1 \frac{a_s^2}{h^2} + c_1 \frac{a_s^2}{h^2} \gamma_0^2 + \dots\right) \quad G'' = G' \tan \delta = G'(\omega\tau_0)^{-1} \quad (8)$$

where $\bar{\sigma}$ is the number of bridges per unit area. The contribution to the storage modulus from loops can be ignored whereas their contribution to the loss modulus is significant.⁶ Consequently, the loss modulus has a poor dependence on the strain amplitude. Because $a_s^2 \ll h^2$, eq 8 states that the strain hardening starts at some constant value of $\gamma_0^2 [a_s/h]^2$. Therefore, at the onset of strain hardening we get

$$\gamma_c \propto \frac{h}{a_s} = [(1 + \xi)^{1-\beta} - 1] \frac{t}{a_s} \quad (9)$$

where γ_c is the strain at the onset of strain hardening.

Thus, the model shows that the strain at the onset of strain hardening is independent of polymer molecular weight and frequency and depends only on the clay concentration.

3. Discussion

We are now in a position to analyze the experiments by Krishnamoorti and Giannelis³ on end-tethered poly(ϵ -caprolactone) (PCL)–montmorillonite (MMT) nano-

composites. The system consists of well-dispersed clay plates in the polymer matrix. Because the polymerization is carried out by an initiator chemically bound to the clay surface, a fraction of the polymer molecules are end-tethered. The remaining fraction is free because of chain-transfer reactions. For our model to be applicable to the experimental system, it should satisfy three conditions. First, there needs to be an attractive interaction between the polymer and the clay surface. Second, the surface coverage of the end-tethered polymer chains on the clay surface should not be very high because it restricts the penetration of the chains external to the tethered layer. Third, the coil size (molecular weight) of the polymer should be greater than the average distance between the opposite clay surfaces.

PCL is known to have a strong affinity for the clay surface.^{7,8} Hyperconjugation of the methylene group in the α position leads to an electronic deficiency resulting in a net positive charge that interacts with the negatively charged clay surface,⁸ thus enhancing the possibility of polymer chains bridging the two plates. To address the second condition, we need to understand the morphology of the polymer chains on the clay surface. The end-tethered polymer-clay nanocomposite²⁻⁴ is prepared by an in situ ring-opening polymerization (ROP) of the cyclic monomer, ϵ -caprolactone. The polymer that originates from this initiator is in principle tethered to the clay. Although one may assume that charge-carrying capacity dictates the surface coverage (number of polymer chains attached per unit area) of the clay plate, it is possible that some initiators do not get activated. Also, the growth of some chains can get curbed to a very small molecular weight, making an effective surface coverage smaller than that dictated by the charge-carrying capacity. Furthermore, the chain-transfer events customary in the ROP terminate the growing chain and initiate another chain.⁹ Therefore, the polymer molecular weight, which should ideally be inversely related to the clay concentration, actually shows only a poor dependence on the clay loading because of the above-mentioned effects.^{3,4}

Let us assume that there are m number of initiator sites, each leading to one end-tethered chain and n number of free chains per unit mass of clay. Then, if there are α chain-transfer events on average per initiator site on the clay surface, then $n = \alpha m$. If the average surface coverage of the end-tethered chains is σ , then we get $m = 2\sigma t/\rho_c$. Furthermore, if a is the length of a monomer unit and if there are N_i monomers in the i th molecule (where i varies from 1 to $m + n$), then the volume of the polymer per unit mass of clay is given by $V_p = a^3 \sum_{i=1}^{m+n} N_i$, and the mass of the polymer per unit mass of clay is given by $\rho_p V_p$. The number-average molecular weight of a polymeric system is given by $M_n = M_0 \sum_{m+n} N_i / (m + n)$, where M_0 is the monomer molecular weight. Let \bar{N} be the average number of monomers per chain ($\bar{N} = \sum N_i / (m + n) = M_n / M_0$). Therefore, the weight percent of the clay is given by

$$\phi = \frac{1}{1 + \rho_p V_p} = \frac{1}{1 + \rho_p a^3 \bar{N} (m + n)} \quad (10)$$

Rearranging eq 10 and incorporating the expression for m , we get

$$\bar{N} a^2 \sigma = \frac{1 - \phi}{\phi} \frac{t \rho_c}{2a \rho_p (1 + \alpha)} \approx \frac{1 - \phi}{\phi} \frac{1}{(1 + \alpha)} \quad (11)$$

with $t \rho_c / (2a \rho_p) = O(1)$.¹⁰ This equation gives us important insight into the morphology of the polymer chains on the

Table 1. Molecular Weight, Its Distribution, and Other Characteristic Features of the Systems Studied by Krishnamoorti and Giannelis³

ϕ	M_n	M_w	M_w/M_n	\bar{N}^b	h/t		X_w^a	
					$\beta = 0.39$	$\beta = 0.23$	$\beta = 0.39$	$\beta = 0.23$
0.03	9200	14470	1.57	81	12.2	24.9	10.8	0.04
0.05	8800	13 550	1.53	77	8.6	16.3	40.1	1.4
0.07	27 647	47 000	1.70	243	6.7	12.3	97.3	61.4
0.1	9900	16 030	1.62	87	5.2	8.9	91.2	41.3

^a X_w : Mass fraction of chains having a coil size greater than h assuming a log-normal distribution. ^b $\bar{N} = M_n/M_0$, where $M_0 = 114$, molecular weight of the monomer unit.

clay plate. It can be seen that the molecular weight of the polymer, surface coverage, number of transfer events in polymerization, and clay concentration are linked to each other. For known values of the clay concentration and the molecular weight, we get a relationship between the surface coverage and the number of transfer events per growing chain. The left side of eq 11 is a product of surface coverage and the square of the radius of gyration of the tethered molecule. For $\bar{N} a^2 \sigma \leq 1$, the neighboring tethered chains do not interact with each other (mushroom regime), whereas for $\bar{N}^{0.5} a^2 \sigma \leq 1$, polymer chains obey the Gaussian configuration.¹¹ For higher surface coverage, $\bar{N}^{0.5} a^2 \sigma > 1$, the brush thickness increases linearly with the molecular weight, and the external polymer chains are almost expelled out of the brush making it "dry".¹¹ It can be clearly seen that for a known clay concentration the higher the number of transfer events per initiator the smaller the value of $\bar{N} a^2 \sigma$ and the greater the number of free chains in the system. In the same regard, flow activation energy measurements by Krishnamoorti and Giannelis⁹ provide an important insight. The flow activation energy of the polymer clay nanocomposite was estimated to be 19 kJ/mol whereas that of homopolymer was estimated to be 17 kJ/mol.⁹ The fact that the two values are almost identical suggests that the contribution of confinement to the relaxation behavior (or self-diffusivity) is minimal.¹² In other words, the chains in the clay gallery are dominated by free chains because if the chains in the gallery were dominated by chemically bound (end-tethered) chains there would have been a substantial increase in the flow activation energy. We believe that the number of transfer events per initiator site is significant enough that $\bar{N} a^2 \sigma < 1$. Thus, the outside polymer chains can enter the brush and get adsorbed on the clay surface. Such adsorption will increase the surface coverage, but we believe that it always remains in the regime $\bar{N}^{0.5} a^2 \sigma \leq 1$ because for higher surface coverage the configurational entropy will decrease. Thus we assume that the configuration of the polymer chain always remains Gaussian in the clay gallery.

Krishnamoorti and Giannelis³ report four nanocomposite formulations with clay concentration varying from 3 to 10 wt %. The molecular weight of the polymer along with its distribution in the four formulations is given in Table 1. To determine if the polymer has sufficient molecular weight to bridge the clay layers, we need to know the interlayer spacing h . However, h is given by eq

- (7) Messersmith, P. B.; Giannelis, E. P. *Chem. Mater.* **1993**, *5*, 1064.
 (8) Gardebien, F.; Gaudel-Siri, A.; Brédas, J.; Lazzaroni, R. *J. Phys. Chem. B* **2004**, *108*, 10678.
 (9) Krishnamoorti R.; Giannelis E. P. *Macromolecules* **1997**, *30*, 4097.
 (10) $\rho_p = 1.2$ g/cc, $\rho_c = 2.5$ g/cc, $t = 0.94$ nm, and $a = 0.87$ nm so that $t \rho_c / (2a \rho_p)$ is of order 1. Brocogens, P. Personal communication, 2004.
 (11) Legér, L.; Raphaël, E.; Hervet, H. *Adv. Polym. Sci.* **1999**, *138*, 185.
 (12) Galgali, G.; Lele, A.; Ramesh, C. *Macromolecules* **2001**, *34*, 852.

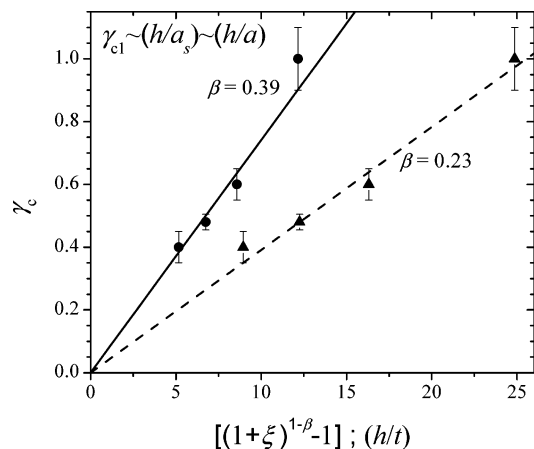


Figure 3. Critical strain at the onset of strain hardening plotted against (h/t) . The points in both data sets are same experimental data for the two values of β , whereas the lines are a linear fit. We get the best linear fits that also pass through an origin for $0.39 > \beta > 0.23$.

1 and requires a determination of β . To facilitate this, we first assume the coil size of the polymer chains to be larger than h . By further assuming affine deformation, we may fit eq 9 to the experimental data to get the value of β .¹³ As described in the model, under LAOS, the bridge elongates and shows strain hardening. Figure 3 shows the critical strain at the onset of strain hardening plotted against $[(1 + \xi)^{1-\beta} - 1]$ for the same experimental data with the two values of β along with the model fit. The best linear fits to the experimental data that also pass through the origin can be obtained for values of β in the range of $0.39 \geq \beta \geq 0.23$. It can be seen from eq 3 that as β decreases h increases. Table 1 shows h corresponding to these two limits for all of the clay concentrations. The proposed range of β is also consistent with the X-ray diffraction analysis that shows the interlayer separation in all of the formulations to be greater than 5 nm.⁴ Assuming a log-normal distribution of the polymer molecular weight, the weight fraction of the polymer chains that possess a Gaussian coil size greater than h for each system is also given in Table 1. For the highest value of β , all samples except the one having 3 wt % clay possesses a significant fraction of chains that can bridge the opposite clay layers. In the system having 3 wt % clay, only a moderate fraction of the

chains possess a coil size sufficient to bridge the two plates. However, for such a low concentration of clay, the distribution in h may be expected to be broad, and it is possible that a larger fraction of chains actually bridge the clay plates. The large error bar for the 3 wt % clay system in Figure 3 also suggests the larger distribution in h . Furthermore, it can be seen that as β decreases smaller and smaller fractions of the polymer chains possess a molecular weight sufficient to bridge the clay layers. Thus for system to show strain hardening, we believe that the value of β is closer to 0.39 so that the distance between the plates is minimal.

Thus, this study suggests some important factors necessary for observing the strain hardening. First, the polymer should have adequately strong affinity with the clay surface, and second, the coil size of a sufficient fraction of the polymer chains should be greater than the distance separating the two plates.

4. Summary

In this work, we have presented a scaling model to analyze the reversible strain-hardening behavior of poly(ϵ -caprolactone)/MMT end-tethered nanocomposites as observed by Krishnamoorti and Giannelis under large-amplitude oscillatory shear.³ Our model is based on the assumptions that the polymer has affinity for the clay surface so that polymer chains that span the distance between the two clay plates would bridge them. As the strain amplitude in the oscillatory shear deformation increases, the bridges are stretched and contribute to the storage modulus, thereby increasing the complex viscosity. The model predicts that the strain at the onset of strain hardening is independent of the frequency of oscillations and the polymer molecular weight but decreased with increasing clay concentration, all of which were experimentally observed by Krishnamoorti and Giannelis.³ The onset of strain hardening thus depends only on the average distance separating the consecutive plates.

Acknowledgment. I thank Professor Morton Denn, Levich Institute, New York, and Professor Ashish Lele, National Chemical Laboratory, India, for several fruitful discussions. I also thank Professor Ramanan Krishnamoorti, University of Houston, for sharing his experience on the current system. Furthermore, I acknowledge my correspondence with Professor Patrick Brocorens, Université de Mons-Hainaut, Belgium, for providing some vital information on poly(ϵ -caprolactone).

LA051568U

(13) In eq 9, because for PCL and MMT $t \approx a$ and $N_s a_s < h^2/a$, we have $t < a_s$.